Wideband Low-Noise HEMT Preamplifier for High-Speed Optical Transmission Systems

G. Torrese*, J.-P. Raskin*, N. Haese**, and A. Vander Vorst*

*Microwave Lab., Université catholique de Louvain, 3, Place du Levant B-1348 Louvain-la-Neuve, Belgium

Fax: +32.10.47.87.05 e-mail: torrese@emic.ucl.ac.be **Institut d'Electronique et de Microélectronique du Nord (IEMN), UMR CNRS 8520, 59652 Villeneuve d'Ascq, France

This paper describes a broadband low-noise preamplifier suitable for 40 Gb/s optical communication systems. To reduce the noise to the absolute minimum, a high impedance front-end, followed by an equalizer, has been designed. The circuit, based on 0.2 µm gate length HEMT technology, was characterized both in terms of bandwidth and noise performance. Measured results demonstrate the great interest of using low-cost wideband HEMT amplifier hybrid coupled to p-i-n photodiodes for OEIC receivers. Despite differences between simulated and measured results due to hard failures during the fabrication, the amplifier achieves a 40 dB trans-impedance gain over 35 GHz of bandwidth.

Introduction

In the last few years the volume of data transmitted over optical fiber links has increased rapidly. At present, systems operating at 20 Gb/s are utilized, while 40 Gb/s time-division multiplexed (TDM) optical transmissions have already been demonstrated [1],[2]. As wideband optical receivers for these systems, monolithic receiver opto-electronic integrated circuits (OEICs) have been investigated [3],[4]. Because of the possibility of reducing parasitics associated with the interconnection between photodetector and amplifier, monolithic OEICs exhibit excellent performance in terms of speed and reliability. It should however be noted that, the monolithic integration represents a significant challenge when trying to optimize different devices grown in a single run.
In this paper, we discuss a broadband low-noise preamplifier covering 44 MHz to 40 GHz, suitable for hybrid integrated optical receivers. In comparison with the monolithic approach, the hybrid integration is more flexible, allowing us to combine different photodetectors with the amplifier.

Circuit design

Optical front-ends for 40 Gb/s transmissions need both a flat frequency response to avoid signal distortions, and a good noise performance to maximize the receiver sensitivity. In order to reduce all the noise sources to the absolute minimum, a high-impedance front-end has been considered. The basic design principle consists of loading the photodiode with an impedance as large as possible. Hence, the photogenerated current is converted into a voltage which is amplified. When increasing the value of the resistor, the voltage dropping at the amplifier input goes up, reducing in this way the amount of noise. Unfortunately, the high-impedance front-end bandwidth is limited by the product between the capacitance at the input amplifier node and the load resistor. Because it is desirable to have large resistor values to reduce the thermal noise, the front-end suffers from an extremely low

cut-off frequency. Consequently, an equalizer high-pass network has been added in order to compensate the low-pass frequency response of the high-impedance front-end.

Fabrication

The circuit has been implemented in a 0.2 μm low-noise *GaAs* pseudomorphic HEMT OMMIC (formerly Philips PML) ED02AH technology. Two normally-off (enhancement mode) transistors have been used. Details of the packaging technology, DC bias and AC signal paths are shown in Fig. 1. In order for signals to go in and out of the monolithic mi-

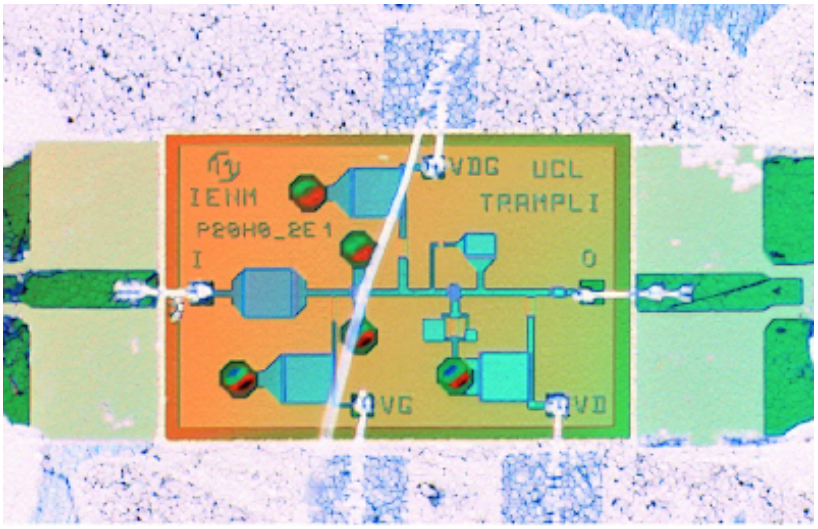

Figure 1: Integrated amplifier view.

crowave integrated circuit (MMIC), input and output pads have been wire bonded. As the resulting stray capacitances and lead inductances can impair the amplifier performance, wire bondings have been minimized by keeping high control over the distance between the MMIC and the alumina mounting substrate. The bias point for the first and second stage transistors has been set by using three external voltage generators. A two-supply approach has then been used to bias the high-impedance front-end. The two-supply configuration allows us to control both the gate-source and the drain-source voltages independently. The equalizer is biased by imposing the drain-ground voltage, while the gate-source voltage depends on the first stage bias. External RF bypass capacitors used to decouple the DC from the AC path have been placed as close as possible to the chip. Finally, both the amplifier and the alumina substrate have then been mounted over a brass housing.

Results

The RF characterization of the amplifier was based on the electrical scattering parameter measurements, between 250 *MHz* and 40 *GHz*. Due to errors during the fabrication process, measurements deviate sensitively from simulations. The main difference concerns the amplifier gain. It is much lower than that expected. Thus, in order to reduce the mismatch between measurements and simulations, the circuit bias voltages have been

Table 1: Operating bias points.

Bias voltages	V_g [V]	V_{dg} [V]	V_d [V]
for simulations	0.5	5.0	6.0
for measurements	0.4	15.0	7.0

opportunely tuned. Both ideal bias used for simulations and the larger bias required to insure broad bandwidth operations are shown in Table 1. The voltage V_g, applied to the gate of the first transistor, results a little bit lower than the theoretical one. On the other hand, V_d, used to bias the drain of the second transistor, and V_{dg}, used to bias both the drain and gate of the first and second HEMTs respectively, are sensitively larger. The use of higher bias voltages is required because of the hard failures which compromise the amplifier operation. By performing new simulations and by measuring the transistor I-V characteristic we show that the normally-off HEMTs exhibit a negative threshold voltage. Consequently, a drain-to-source current already flows for a zero gate-to-source voltage. Moreover the resistivity of the active layer is out of specification.
A comparison between simulated and measured response for the optical receiver is shown in Fig. 2(a). A simple *p-i-n* photodiode model, taking into account junction capacitance (C_j = 50 fF), series resistance (R_s = 30 Ω), and bonding inductance (L_s = 2 nH) has been used to determine the overall frequency response. As can be seen, although the optimal response has been compromised by hard failures, occurred during the amplifier fabrication, the measured curve approaches that simulated. Unfortunately, it is not as flat as desired.

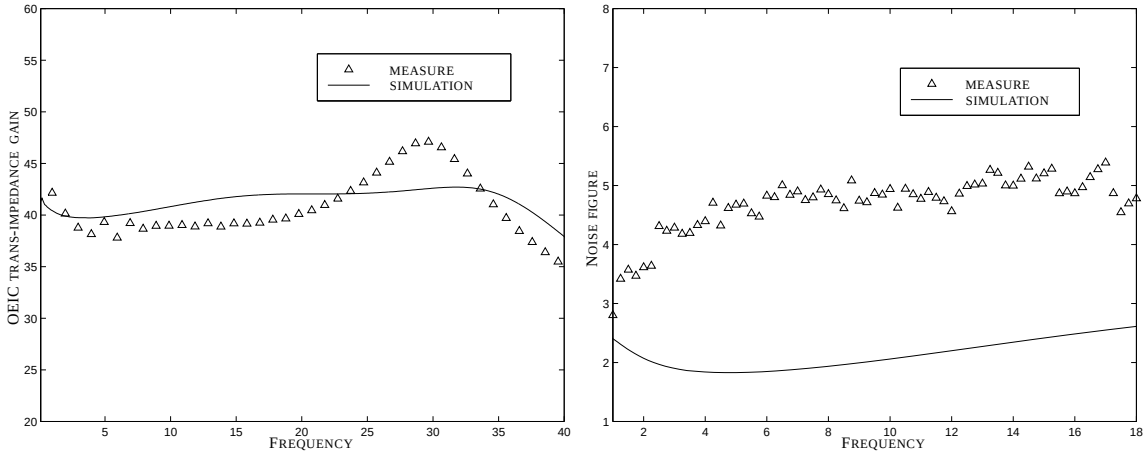

(a) (b)

Figure 2: Comparison between measured and simulated receiver bandwidth (a) and measured and simulated amplifier noise figure (b).

The amplifier noise performance was determined in terms of noise figure. It represents the degradation in the signal-to-noise power ratio when a current (or a voltage) at the amplifi-

er input is passed through it. Simulated and measured noise figure from 1 *GHz* to 18 *GHz* are shown in Fig. 2(b). Simulated results have been obtained by using the optimal bias point calculated theoretically, while measurements correspond to a higher bias voltage, used to guarantee wide bandwidth operations. As both the induced gate noise current and the channel noise current depend on the applied external voltage, large biases increase the amount of noise degrading the amplifier sensitivity. Consequently, the measured noise figure is larger than the simulated one. It is possible to show that the lowest noise is obtained for relatively low values of the drain-to-source voltage, where the gain begins to saturate. A further increase of the drain bias determines only worse noise performances. On the other hand, for a given drain-to-source voltage, there is an optimal gate-to-source voltage which allows us to minimize the channel noise.

Conclusions

We have designed, fabricated and characterized a wideband amplifier operating in the range 44 *MHz*-35 *GHz* with 40 *dB* trans-impedance gain. Although hard failures compromise the fabrication process, the difference between simulations and measurements has been minimized by increasing the bias voltages. Unfortunately, as both the drain-to-source voltage and the gate-to-source voltage strongly affect the noise performance, the difference between simulated and measured noise figures increases when increasing the amplifier bias operation points. On the base of scattering parameter measurements, a hybrid integrated photoreceiver using a *p-i-n* detector has been simulated, demonstrating the possibility of utilizing the amplifier in very high bit-rate optical fiber communication systems.

Acknowledgment

This work is partially funded by project PAI-IV/13 of the Belgian Federal Office for Scientific, Technical and Cultural Affairs.

References

[1] W. Bogner, E. Gottwald, A Schopflin, and C.-J. Weiske, " 40 $Gbit/s$ unrepeatered optical transmission over 148 *km* by electrical time division multiplexing and demultiplexing", *Electron. Lett.*, vol. 33, pp. 2136-2137, 1997.

[2] E. Gottwald, A. Felder, H.-M. Rein, M. Möller, M. Wurzer, B. Stegmüller, M. Plihal, J. Bauer, F. Auracher, W. Zirwas, U. Gaubatz, A. Ebberg, K. Drögemüller, C. Weiske, G. Fischer, P. Krummrich, W. Bogner, and U. Fischer, " Toward a 40 Gb/s electrical time division multiplexed optical transmission system", in *ICCT'96*, Beijing, China, , pp. 60-63, May 1996.

[3] M. Bitter, R. Bauknecht, W. Hunziker, and H. Melchior, " Monilithic *InGaAs-InP p-i-n* 40 $Gbit/s$ Optical receiver Module", *IEEE Phot. Technol. Lett.*, vol. 12, no. 1, pp. 74-76, Jan. 2000.

[4] G.G. Mekonnen, W. Schlaak, H.-G. Bach, R. Steingrüber, A. Seeger, Th. Enger, W. Passenberg, A. Umbach, C. Schramm, G. Unterbörsch, and S. van Waasen, "37-*GHz* Bandwidth *InP*-Based Photoreceiver OEIC Suitable for Data Rates up to 50 Gb/s", *IEEE Phot. Technol. Lett.*, vol. 11, no. 2, pp. 257-259, Feb. 1999.